

8-BB

Experimental Study of Erosion Resistant Materials for Use in Diverter Components

by

Principal Investigator: Adam T. Bourgoyne, Jr., Ph.D.
Associate Researchers: Alok Jain
O. Allen Kelly
*Petroleum Engineering Department
Louisiana State University
Baton Rouge, LA 70803-6417*

May 26, 1995

"This study was funded by the Minerals Management Service, U.S. Department of the Interior,
Washington, D.C., under contract Number 14-12-0001-30441."

The views and conclusions contained in this document are those of the authors and should not be interpreted as necessarily representing the official policies or recommendations of the Department of the Interior.

Experimental Study of Erosion Resistant Materials **For Use in Diverter Components**

Principal Investigator : Dr. Adam T. Bourgoyne, Jr.
Associate Researchers : Alok Jain
O. Allen Kelly
Petroleum Engineering Department,
Louisiana State University,
Baton Rouge, Louisiana 70803-6417

Abstract

A diverter is a safety device used on oil and gas drilling rigs as a means of handling shallow gas flow. A common mode of failure of the diverter is erosion of the bends in the surface vent lines that divert the flow away from the rig.

The objectives of the study carried out at LSU were to identify new or alternate materials that are more resistant to sand erosion than those that are currently being used in the field, thereby enhancing diverter system operational safety; and to obtain sufficient experimental data to allow estimation of life of a component that is used to make a bend in a diverter system.

Work done includes experiments on low carbon steel flat plates and various other erosion resistant materials by maintaining sonic velocity of the carrier fluid. Study of the effects of various parameters such as angle of impact and rate of sand flow on the erosion rates of these materials was also carried out.

Low carbon steel of A-36 specifications had the maximum erosion rate when blasted with sand grain size of US mesh # 80-120 at an impact angle of thirty degrees. Stellite 6K showed the least erosion rate among the materials tested under similar conditions. When the angle of impact was changed to ninety degrees, keeping all the other parameters the same as before, low carbon A-36 steel showed the maximum erosion rate once again and the performance of stellite 6K remained near the best of the materials tested. Comparing the erosion performance of these materials at different angles indicates that erosion is a greater problem at thirty degrees than at ninety degrees. It was found that the life of a diverter component could be increased by almost 100% if it is coated with stellite 6K over the use of uncoated low carbon A-36 steel.

Introduction

Blowouts are among the most dangerous hazards of oil and gas exploration. When a well threatens to blowout, the prompt use of properly designed blowout prevention equipment is necessary to avoid harm to personnel and loss of the drilling structure. Well control is especially

difficult when a threatened blowout situation occurs at a shallow depth. During the course of drilling operations, periods often exist when the well should not be closed on a threatening blowout as the formation is not competent enough to keep an underground blowout from breaching to the surface. When a threatened well blowout situation occurs and none of the other conventional methods of controlling the well can be used, a diverter system must be used.

A diverter system is a safety device used on oil and gas drilling rigs to direct uncontrolled flow of formation fluids away from the rig. This system is composed of some means for changing the direction of flow from vertical to horizontal, usually with an annular packing element, and a pipe system that leads the flow away from the rig. The essential elements of a diverter system include a vent line for directing flow away from the rig, a means for closing the well annulus above the vent line during diverting operations, and a means for closing the vent line during normal drilling operations.

The diverter must function for at least enough time to allow for an orderly evacuation of rig personnel. The past performance of diverter systems has been very poor. Failures have been caused by excessive pressure losses through the diverter system, operational problems with valves, and erosion of valves and vent lines. The use of larger vent sizes and selection of an appropriate conductor casing depth can reduce the risk of high back pressure. Proper selection of diverter valves and valve operations, followed by periodic maintenance and testing, can eliminate operational problems with valves.

It has been observed that a common cause of diverter failure is erosion. Erosion can be caused by cavitation and by impingement of liquid or solid particles. Erosion by impingement of solid particles is most rapid and therefore it is of primary concern for diverter operations. A specific erosion factor, F_e , is often used to express the erosion caused by particle impact. This factor is defined as the mass of steel removed per unit mass of abrasive. Erosion occurs predominantly at points where the flow changes direction, such as a bend in the diverter. A straight diverter vent line is always the preferred choice but turns in the vent lines are sometimes unavoidable when a diverter is installed on an existing rig due to the equipment layout.

Previous Work

In the past, several investigators studied the effects of varying impact angle, particle velocity, particle mass, and properties of the abrasive particle and target materials on erosion rate.

The majority of experimental work to investigate the effects of impacting velocity on erosion rate has proven erosion rate to be proportional to velocity raised to the second or third power. The study by Finnie (1967) found the velocity exponent to be between 2.48 and 2.69 when the target was annealed SAE 1215 steel. The effect of velocity on erosion rate is shown below.

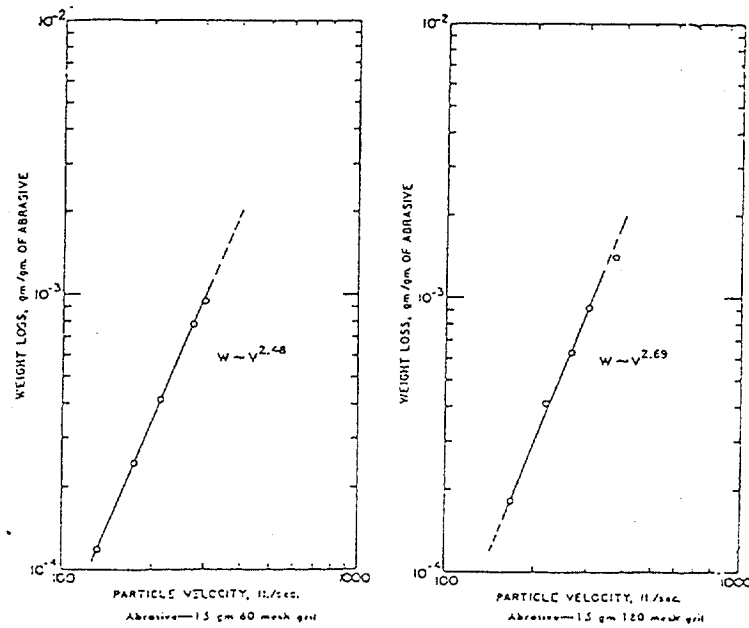


Figure 1: Effect of velocity on specific erosion of annealed SAE 1215 steel, 20 degrees impact SiC (from Finnie 1967)

Ives and Ruff (1978) found that erosion rate for a ductile material was maximum at an impact angle of about 20 degrees while brittle materials underwent maximum erosion at normal angles of attack. Figure 2 shows the effect of angle of impact on erosion rates.

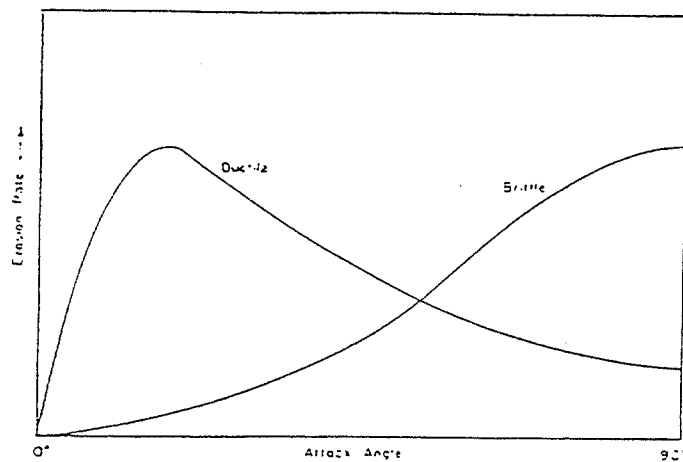


Figure 2: Influence of attack angle on erosion rate (from Ives and Ruff 1978)

Goodwin (1969) showed that at a given particle velocity, erosion rate does not increase with increasing particle size above some minimum particle size. Figure 3 depicts the effect of particle size on the erosion rate.

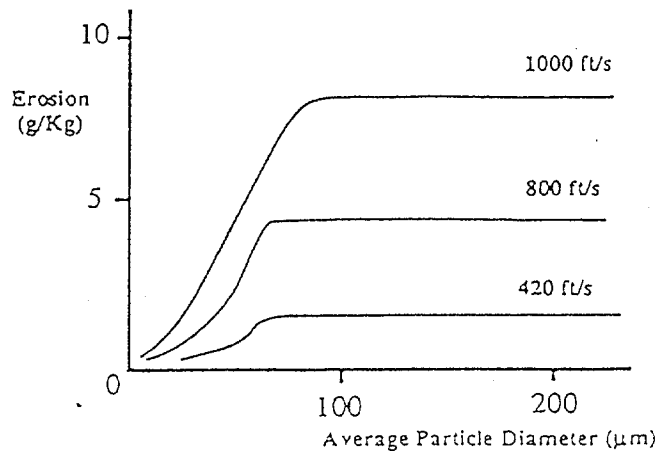


Figure 3: Effect of particle size on specific erosion 11% chromium steel (from Goodwin et. al. 1969)

Previous work conducted at the LSU Petroleum Engineering Research and Technology Transfer Laboratory, experimentally determined the specific erosion factors (F_e) of various fittings affected by abrasives in mud, gas, or mist flows. The fittings evaluated included steel elbows, plugged tees, vortex elbows, and rubber hoses. This work resulted in the development of erosion coefficient correlations for abrasives transported by mud, gas, or mist. A schematic of a model used at LSU for gas-water-sand mixtures is shown in figure 4.

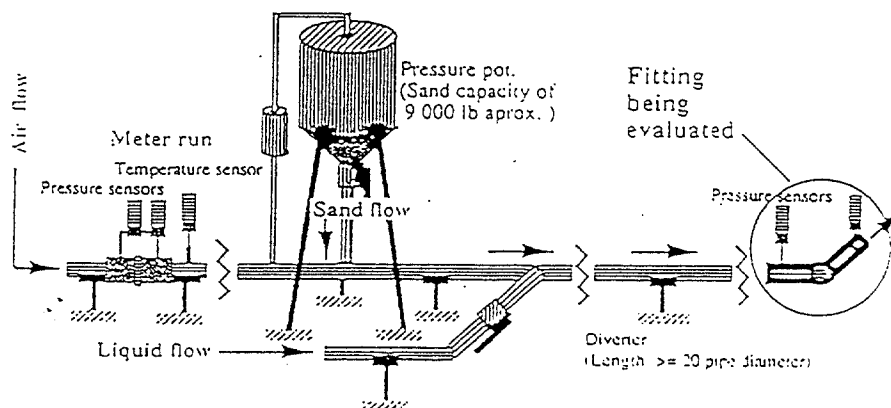


Figure 4: Schematic of a model diverter system for erosion tests

The effect of injecting water directly into the diverted gas flow stream as a means of minimizing the erosion capability of the abrasives contained within the gas flow stream was also studied as part of the previous research work. This work led to the conclusion that water injection does lower the rate of erosion but at the same time increases the pressure at the casing seat. Another finding of the study was that the specific erosion factor is not significantly affected by water content when gas is the continuous phase. It was also observed that external cooling of erosion target zones is not an effective means for reducing the rate of erosion.

Erosion Rate Equation

Based on the previous experimental work carried out at LSU, two equations were proposed for estimating the rate of loss in wall thickness for various fittings; one is recommended for gas and the other for liquid as a continuous fluid carrying abrasive solids.

Dry Gas or Mist Flow

The loss in thickness, h_w , with time, t , of a fitting in a diverter system where gas or mist is the transporting fluid, is given by the following expression in SI units :

$$\frac{dh_w}{dt} = F_e \frac{q_a}{A} \left[\frac{\rho_a}{\rho_s} \right] \left[\frac{u_{sg}}{(u_{ref} \lambda_g)} \right]^2 \quad \dots (1a)$$

where F_e is the specific erosion factor, ρ_s is the density of the diverter system's component, ρ_a is the density of abrasive material, q_a is the flow rate of abrasives, A is area of cross section, u_{sg} is the superficial gas velocity, u_{ref} is a reference velocity of 100 m/s, and λ_g denotes the gas volume fraction.

Liquid Flow

The loss in thickness, h_w , with time, t , of a fitting in a diverter system where liquid is the transporting fluid is given by the following expression in SI units:

$$\frac{dh_w}{dt} = F_e \frac{q_a}{A} \left[\frac{\rho_a}{\rho_s} \right] \left[\frac{u_{sl}}{(u_{ref} \lambda_l)} \right]^2 \quad \dots (1b)$$

where u_{sl} is the superficial liquid velocity, and λ_l denotes the liquid volume fraction.

The above equations calculate the erosion rates based on average superficial carrier reference velocity of 100 m/s. We can modify these equations to calculate the erosion rates at sonic velocity of abrasives as :

$$\frac{dh_w}{dt} = F_{ae} \frac{q_a}{A} \left[\frac{\rho_a}{\rho_s} \right] \quad \dots(2)$$

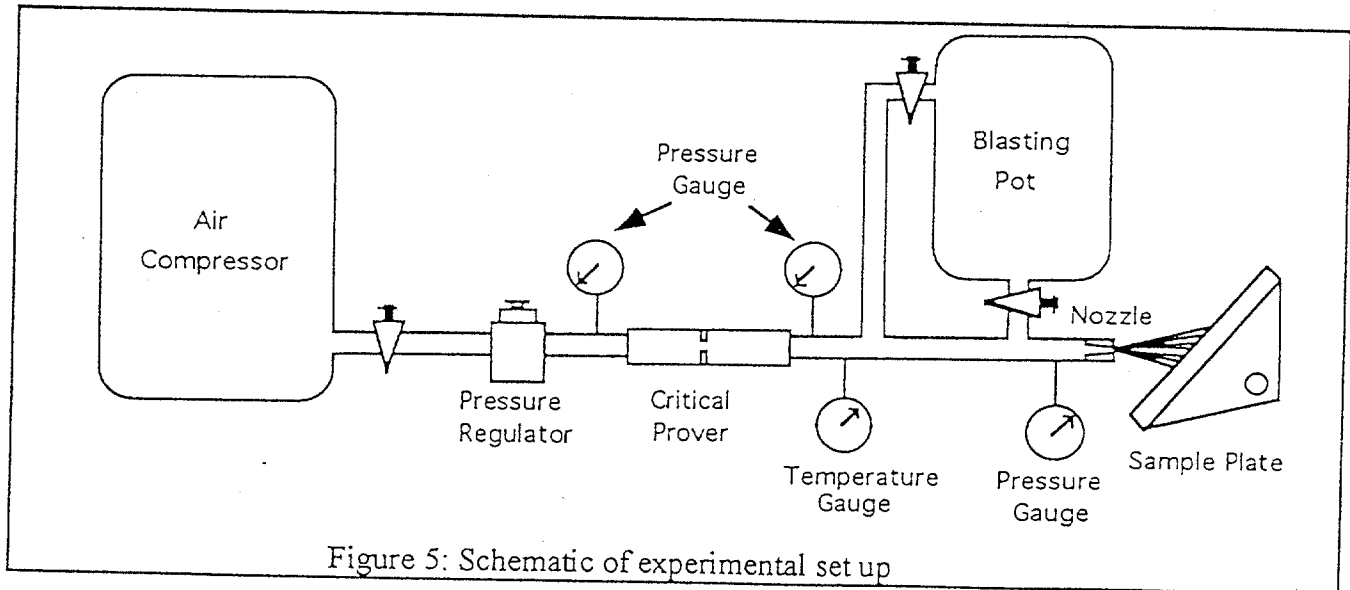
where F_{ae} is the apparent specific erosion factor.

In the previous LSU studies, specific erosion factors of various fittings were determined from experimental data obtained at sub sonic velocities ranging from 32 to 222 m/s. The recent work was performed at sonic velocity of carrier fluid (air in this case) which allowed us to investigate the effect of varying impact angle of abrasive on the erosion rates of flat plates. In addition, the effects of sand grain sizes and sand flow rates on erosion rates were also studied. A comparative study of the erosion rates of various erosion resistant materials was carried out and specific erosion factors (F_e) and apparent specific erosion factors (F_{ae}) for these materials were calculated.

All the previous studies carried out at LSU used common oil field ell and tee fittings made of seamless carbon steel, ASTM-234 grade WPB which was inexpensively available. Since the materials tested in the recent work were expensive, only small size specimens could be used for the tests.

Experimental Equipment and Procedure

The set-up fabricated to carry out the study is shown in figure 5. It consists of an air compressor, a pressure pot for sand injection, a 3/16" critical prover for monitoring gas flow rate, an air pressure regulator, a nominal two inch flow line, and a 1/4" nozzle for maintaining sonic velocity of abrasive stream at the exit.



In addition to this an experimental set-up was fabricated for varying the angle of impact of abrasive on coupons. For economic and safety reasons, the gaseous fluid used in these experiments was air rather than natural gas. Thus an abrasive mixture of air and sand was used to erode the flat plates. Since the coupons provided by Hydril Inc. were expensive, the experimental set-up was first tested by eroding ASTM A-36 specification steel plates which were readily and inexpensively available. Later on, the tests were carried out on the coupons sent by Hydril Inc.

The experimental set-up and procedure was designed to evaluate the rate of erosion and the specific erosion factor of flat plates at different angles of impact of abrasive. The test matrix that was designed focused on evaluating the effect of:

- a) The material selection;
- b) Angle of impact; and
- c) Sand flow rates.
- d) Sand grain size

We maintained air rate at a certain value for all the experimental runs. The weight of the pressure pot was continuously monitored, and sand flow rate was determined from the rate of change in the weight of the pressure pot with time. The mixture of air and sand flowed through a 2" rubber hose and exited through a 1/4" nozzle for five minutes during each run. Weight loss and coupon thickness were determined after the tests. Thickness profiles of the coupons were determined using a dial indicator accurate to 0.001 inch. Grain size distributions of regular blasting sands were measured by sieve analysis. Data were collected to permit evaluation of the effect of change in the angle of impact, sand grain size, sand flow rate, and material type on the erosion rates. Two runs for each set of readings were carried out to check for data reproducibility.

In previous LSU studies, some difficulty was experienced in maintaining a constant sand rate during each test. In this study we were able to maintain sand flow rate at a constant value by installing an orifice in the section of pipe between the blasting pot sand outlet port and the pipe supplying air.

Test Results and Data Analysis

In order to study the effects of the various parameters, specific erosion factor (F_e) and apparent specific erosion factor (F_{ae}) for each run were calculated. Specific erosion factor was obtained as a ratio of loss of weight of the coupon to the mass of abrasives used. The apparent specific erosion factor was calculated from equation (2) proposed for sonic velocity of the abrasive mixtures.

Effect of Angle of Impact on Erosion Rate

The first angle at which the experiment was performed was ninety degrees and the angle was lowered in steps of ten-degrees to fifty degrees. After that, the angles were lowered in steps of five-degrees to twenty degrees. In an effort to find the flow angle at which the observed erosion rate was maximum, additional tests were completed in two-degrees steps between the two tests showing the highest rate of erosion.

Table A1 of the appendix tabulates the test data collected for defining the effect of the impact angle on erosion rates of flat steel plates ASTM A-36 specification. Figure 6 depicts the results in graphical form.

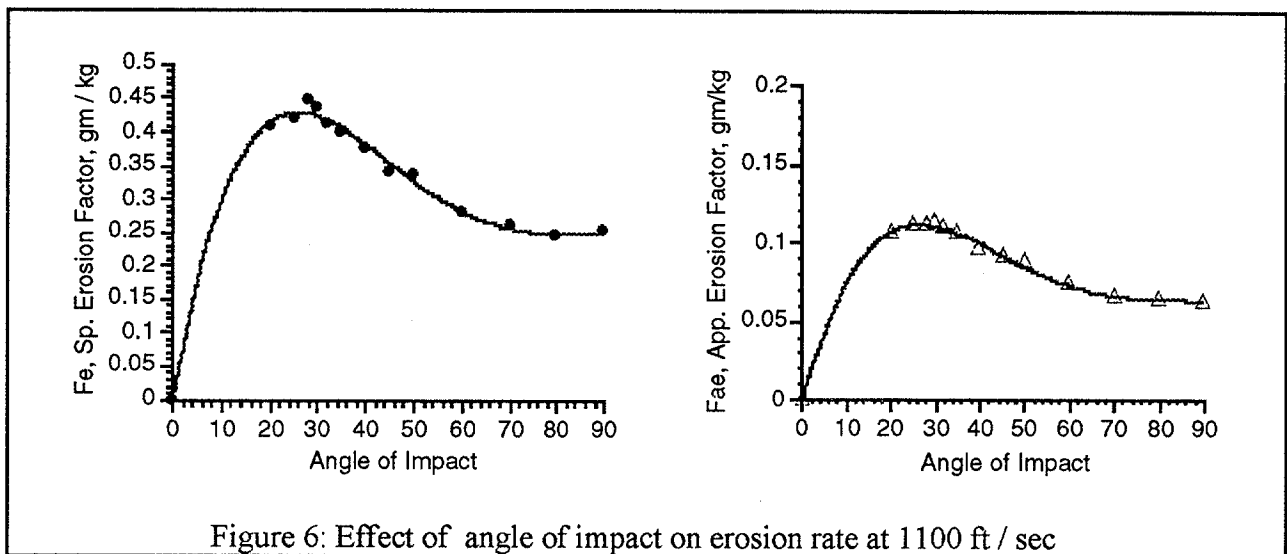


Figure 6: Effect of angle of impact on erosion rate at 1100 ft / sec

As can be observed, the steel plates undergo large erosional losses under glancing angles of impact. Maximum erosion in steel occurred at an impingement angle of thirty degrees. Erosion increases from a ninety-degree angle of impact to thirty degrees. Erosion decreases rapidly for impact angles from thirty degrees through zero degrees. This set of tests shows that the response of steel plates to changes in angles of impact with respect to a stream of high velocity sand particles and air, is typical of ductile materials.

Effect of Sand Rate on Erosion Rate

Different sand flow rates were obtained by installing orifices of different sizes in the section of pipe between the blasting pot sand outlet port and the pipe supplying air. The angle of impact was thirty degrees during this set of runs because maximum erosion was previously observed at this angle. The air flow rate was maintained at 90 scf/min, which was sufficient to produce sonic velocity at the exit. The exit pressure was between 22 and 34 psig over all of the experimental runs.

Table A2 of appendix tabulates the results obtained to define the effect of sand flow rate on erosion. As these results indicate, the wear rate was directly proportional to the sand rate for the range of sand flow rates studied. However, the specific erosion factor shows an inverse relationship to the sand rate. Figure 7 shows the proportional behavior of specific erosion factor with respect to sand rate. Due to limited capabilities of air compressors used, we found it difficult to study the effect of sand flow rate higher than 19 lbs/min. But the sand rates obtained for the tests were sufficient to result in sand concentrations of up to 0.41%, which are acceptable for sand concentrations representative of diverter operating conditions. As the particle concentration in the flow stream increases, the interference between sand grains increases, resulting in the decrease of the specific erosion factor.

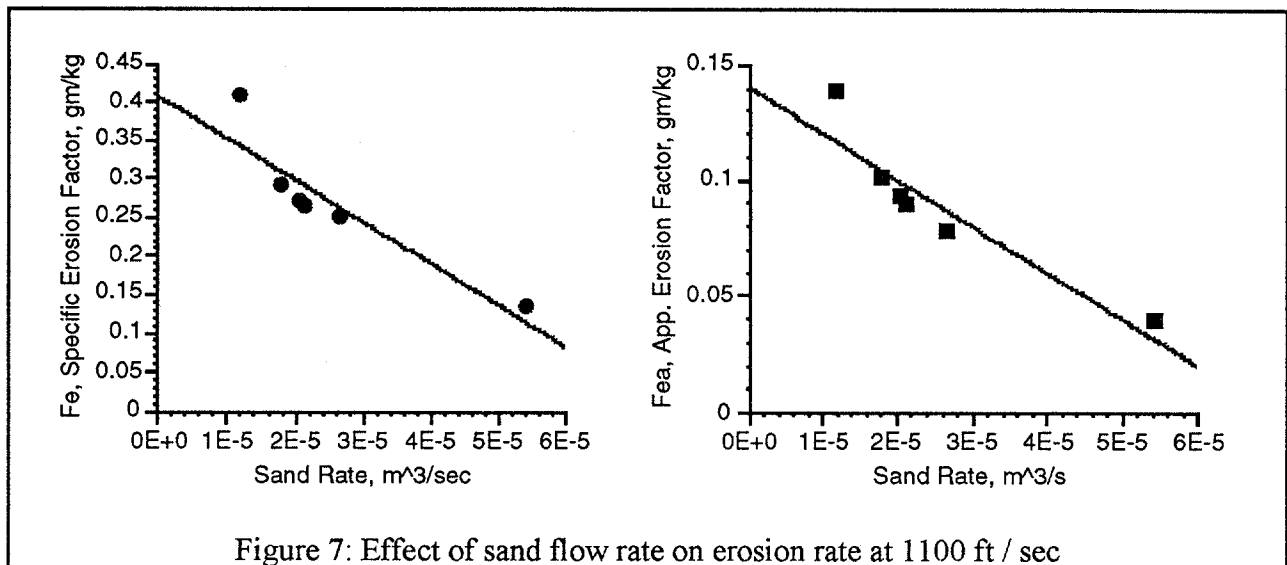


Figure 7: Effect of sand flow rate on erosion rate at 1100 ft / sec

Effect of Sand Grain Size on Erosion Rate

While conducting the tests to study the effects of sand grain size on erosion rate, difficulties were encountered in maintaining constant sand flow rates for different sand grain sizes. In order to keep sand flow rates constant, a series of runs were carried out. Only those observations that had sand rates in the range of 7.125 lbs/min \pm 10 % were taken into consideration.

Contrary to the results of studies by Goodwin (1969), impact of sand grain size of 74 μ m (US mesh # 200) resulted in higher erosion rate than that of sand grain size of 177-124 μ m (US mesh # 80-120). Erosion rates for sand of 1190-420 μ m (US mesh # 16-40) and 500-177 μ m (US # 35-80) showed almost the same value of specific erosion factors. To ensure the repeatability of the results, a second series of runs was carried out and similar results were observed.

Table A3 of appendix tabulates the results obtained during the tests for studying the effect of sand grain size on erosion rate. These results are shown graphically in figure 8.

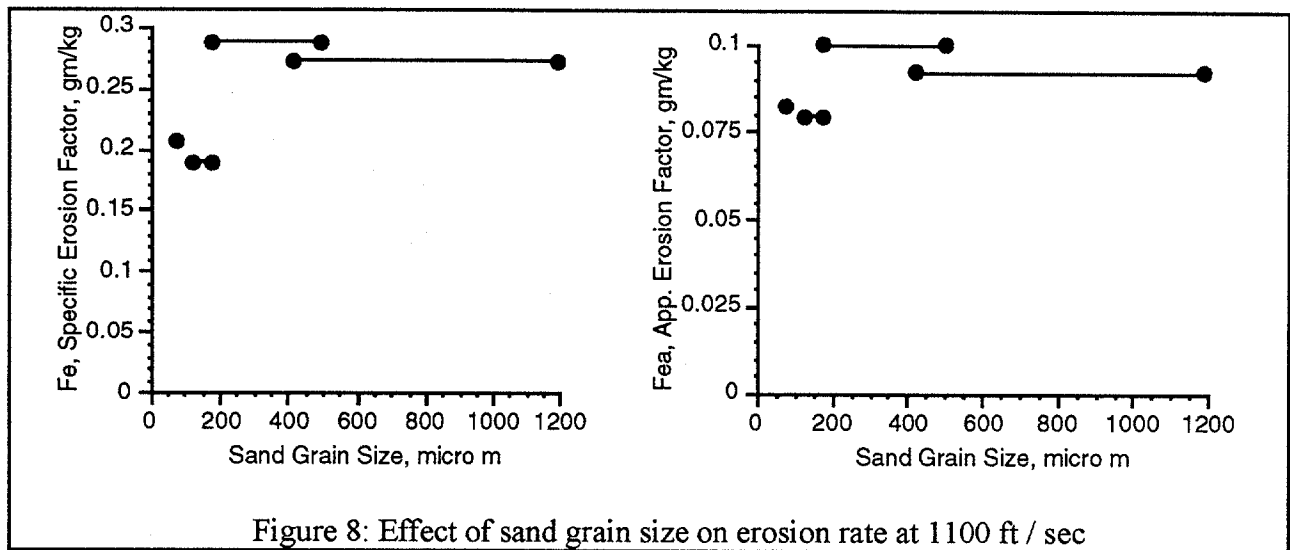


Figure 8: Effect of sand grain size on erosion rate at 1100 ft / sec

Effect of Nozzle Distance from Target on Erosion Rate

In an effort to study the effect of nozzle distance from target, distances between the nozzle and flat plates were varied from zero to three inches keeping the angle of impingement at thirty degrees, air flow rate at 91 scf/min, and sand flow rate at about 4.15 lbs/min.

As the distance between the nozzle and the flat plate was increased from zero to about 1.5 inches, the erosion rate showed an increase since the interference between sand particles decreases. It was also observed that the erosion rate decreased if the distance between the nozzle and the flat plate increased further than 1.5 inches due to reduced impacting velocity of sand particles. The results of these experiments are tabulated in table A4 of appendix.

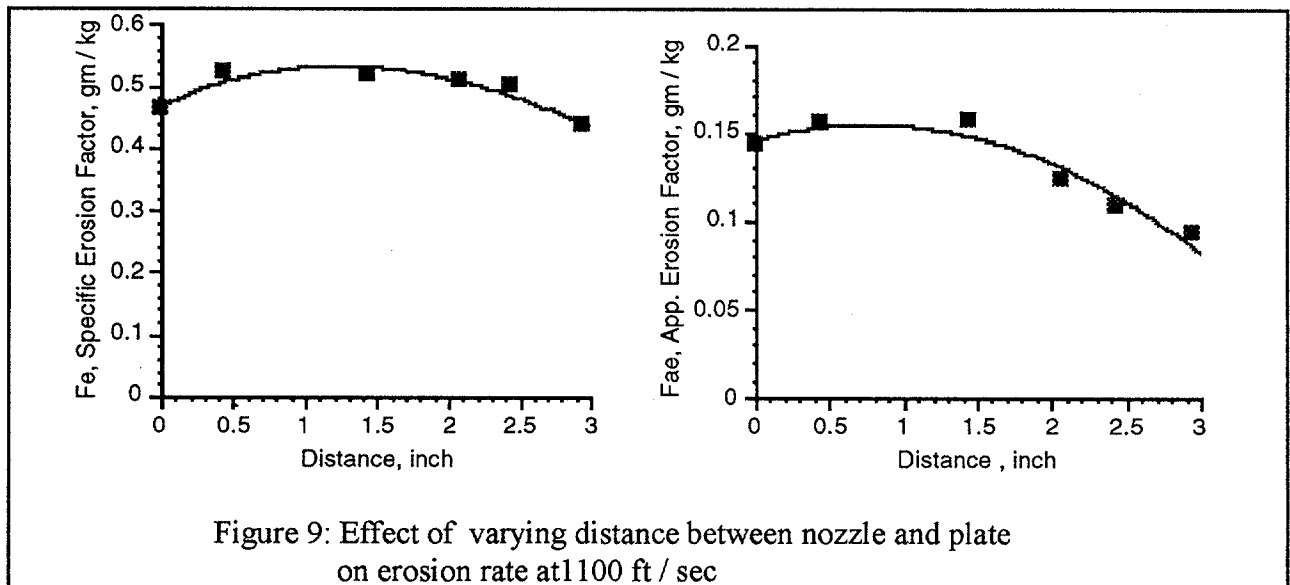


Figure 9: Effect of varying distance between nozzle and plate on erosion rate at 1100 ft / sec

Comparison of Erosion Rates of Erosion Resistant Materials

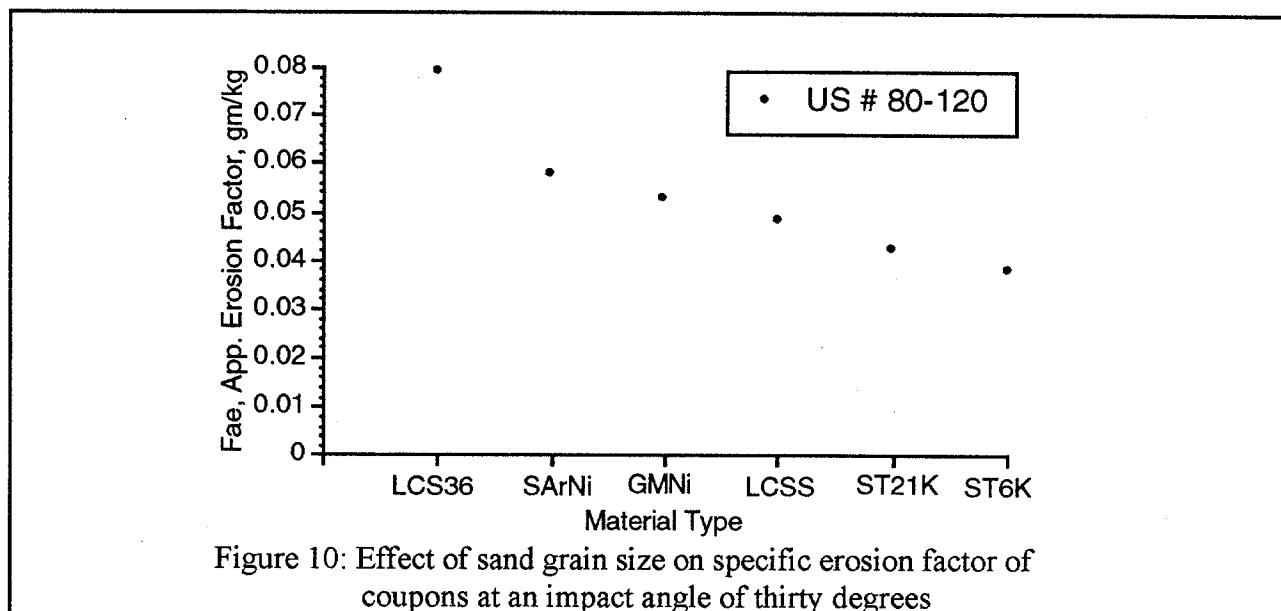
Experiments conducted previously by Bitter (1963 a and b) and Ives and Ruff (1978) showed that ductile materials exhibit maximum erosion rate at impact angles between 20-30 degrees, while brittle materials are least erosion resistant in the vicinity of 90 degrees of the impact angle. In order to differentiate the erosion resistant materials tested in our experimental runs by their degrees of ductility or brittleness, it was decided to carry out tests at the impact angles of ninety degrees and thirty degrees.

In order to facilitate the graphical representation of the results, the materials tested are designated by alphabetical letters as :

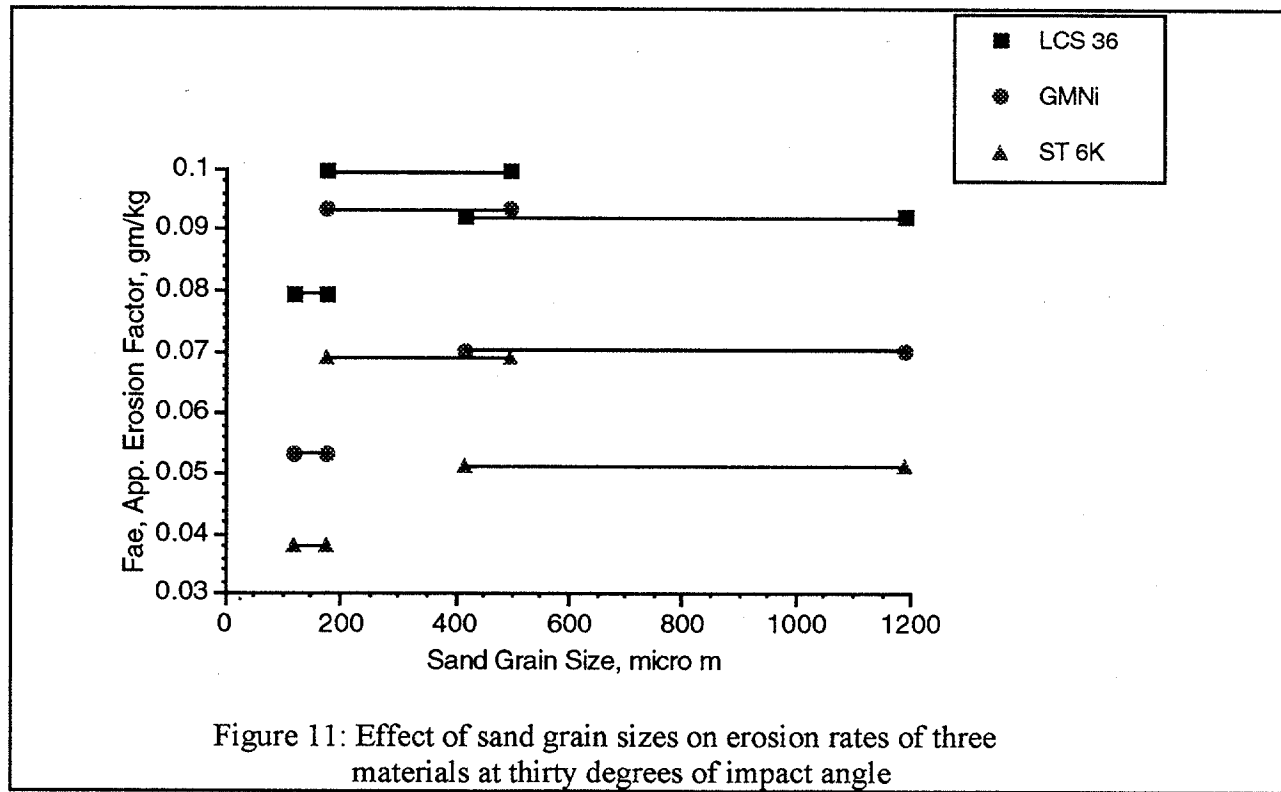
Gas metal arc pulse welding of UNS N 06625 alloy	→	GMNi
Submerged arc welding of UNS N 06625 alloy	→	SArNi
Low carbon stainless steel (UNS S 30603 alloy)	→	LCSS
Stellite 21 K	→	ST21K
Stellite 6 K	→	ST6K
Low carbon steel A-36 specification	→	LCS36

a) At Thirty Degrees of Impact Angle

The angle of impact was changed to thirty degrees keeping the air flow rate at about 90 scf/min. The sand grain size used for blasting the coupons was 300 μm (US mesh # 16-40). It was observed that the submerged arc welding coupon of UNS N 06625 alloy was least resistant to erosion while Stellite 6 K coupon showed the maximum resistance in comparison to other materials tested. Figure 10 shows the apparent specific erosion factors of different materials at thirty degrees of impact angle and US mesh # 80-120 sand which is representative size of sand coming out from a blowing well at sonic velocity at diverter exit.



This general trend, as shown in figure 11, was also evident when the experimental runs were carried out with sand grain sizes of US mesh # 16-40 and 35-80. Thus, apparent erosion factors of different materials are independent of the sand grain sizes used. Table A5 tabulates the results of the experiments conducted to study this effect.

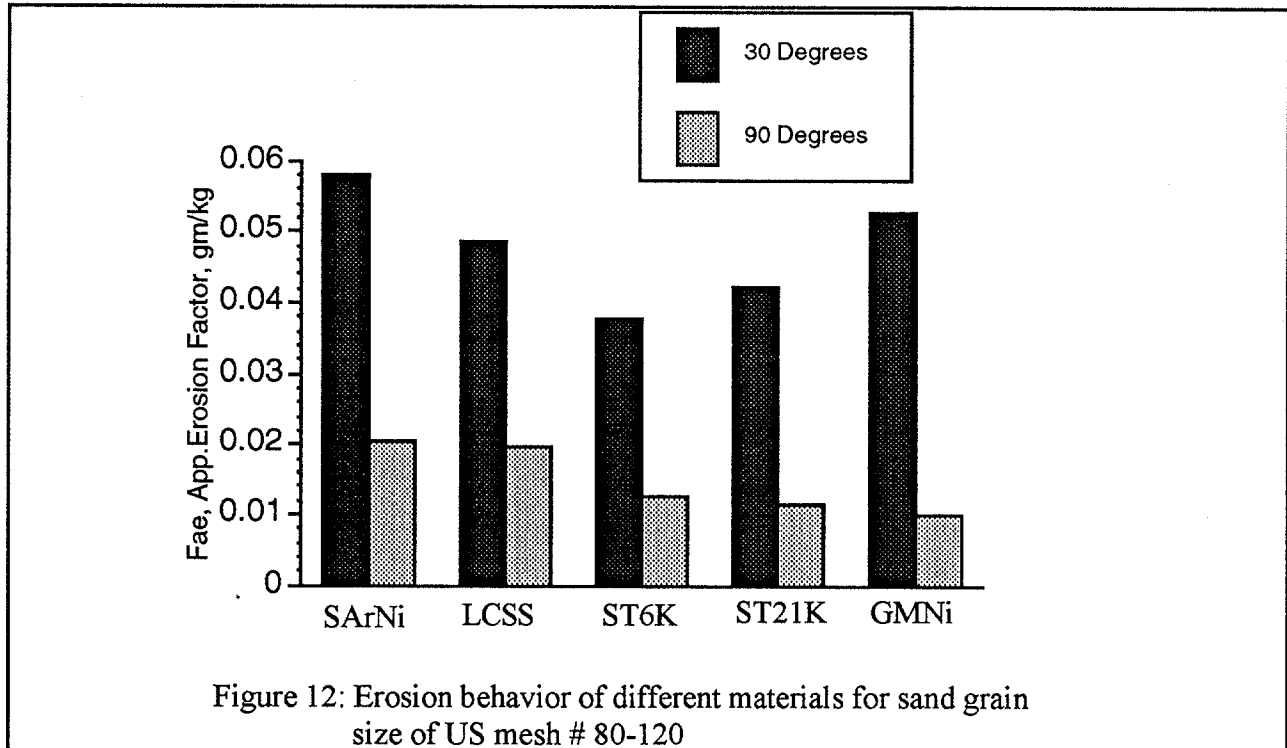


Data show that stellite 6K coating on a component used to make a bend in a diverter would result in increasing its life by almost 100% over a component made of low carbon steel A-36 specifications, when blasted with sand of US mesh # 80-120 (177-124 μm).

b) At Ninety Degrees of Impact Angle

The angle was changed to ninety degrees keeping the air flow rate at about 90 scf/min. It was noticed that low carbon steel A-36 specification showed the highest erosion rate for sand grain size of US mesh # 16-40 (1190-420 μm). If the erosion behavior of various materials to the sand grain size of US mesh # 80-120 (which is representative of sand size from a blowing well) is analyzed, it is observed that submerged arc welding of UNS N 06625 alloy has the maximum while gas metal arc pulse welding of UNS N 06625 alloy has the least erosion rate. This trend, although not well defined, was also evident when the experimental runs were carried out with sand grain sizes of US mesh # 35-80 (500-177 μm) and # 16-40 (1190-420 μm). Similar results were observed when the coupons were blasted at two different sand flow rates suggesting that this behavior is independent of the sand flow rates.

The results are tabulated in table A6 of the appendix. Figures 12 shows that the erosion rates of all the materials tested were less at ninety degrees than at thirty degrees of impact angle suggesting that problem of erosion failure would be more pronounced for all these materials at thirty degrees of impact rather than ninety degrees.



Summary and Conclusions

Experimental data were obtained for studying the effects of angle of impact, sand grain size, and sand flow rate on the erosion rates of low carbon steel A-36 specification plate at sonic velocity of the carrier fluid (air in this case). Experiments were also conducted to make a comparative study of the erosion rates of the erosion resistant materials provided by Hydril, Inc. for sand grain size of US mesh # 80-120.

The conclusions drawn from this study are:

1. Erosion in diverters can be eliminated to a large extent by avoiding bends in the diverter components but these bends in the diverter lines are often unavoidable. It was observed that erosion is a bigger problem at thirty degrees of impact angle than at ninety degrees. Therefore, fittings like plugged tees should be preferred to short radius ells or elbows wherever possible.
2. At thirty degrees of impact angle and sonic velocity at the diverter exit, life of a diverter bend could be increased by almost 100% if it is coated with stellite 6K than with low carbon steel A-36 specification.
3. The erosion resistant materials in the increasing order of erosion rates at thirty degrees of impact angle (long radius ells or elbows with thirty degrees of change in angle) are:
 - a) Stellite 6 K,
 - b) Stellite 21 K,
 - c) Low carbon stainless steel (UNS S 30603),
 - d) Gas metal arc pulse welding of UNS N 06625 alloy,
 - e) Submerged arc welding of UNS N 06625 alloy. and
 - f) Low carbon steel A-36 specification.
4. The erosion resistant materials again in the increasing order of erosion rates at ninety degrees of impact angle (L bends or plugged tees) are:
 - a) Gas metal arc pulse welding of UNS N 06625 alloy
 - b) Stellite 21 K,
 - c) Stellite 6 K,
 - d) Low carbon stainless steel (UNS S 30603),
 - e) Submerged arc welding of UNS N 06625 alloy, and
 - f) Low carbon steel A-36 specification.
5. Erosion rates of steel plate were maximum at thirty degrees of angle of impact. The rate decreased as the angle of impact was increased to ninety degrees.

6. Wear rate increased while specific erosion factor and apparent specific erosion factor decreased with increase in sand concentration in the flow stream.

Acknowledgments

The authors wish to express thanks to Mr. Joe Roche and Mr. R.P. Badrak of Hydril Incorporation for assisting in selecting materials for testing and providing samples.

This research work was supported by the U.S. Minerals Management Services, Department of the Interior. Without their support this work would not have been possible. However, the views and conclusions contained in this document are those of the authors, and should not be interpreted as necessarily representing the official policies, either expressed or implied, of the U.S. Government.

Nomenclature

A	-	Cross sectional area, m^2
f_g	-	Fractional volume of gas
F_e	-	Specific erosion factor, gm/kg
F_{ae}	-	Apparent erosion factor, gm/kg
h_w	-	Thickness, m
q_a	-	Flow rate of abrasives, m^3/s
u_{sg}	-	Superficial gas velocity, m/s
u_{sl}	-	Superficial liquid velocity, m/s
ρ_a	-	Density of abrasives, kg/m^3
ρ_s	-	Density of steel or wall material, kg/m^3
t	-	Time, s

References

1. Badrak, B. 1994, Private Communication.
2. Bitter, J.G.A. 1963 a " A Study of Erosion Phenomena, Part I, Wear 6, pp. 5-21.
3. Bitter, J.G.A. 1963 b " A Study of Erosion Phenomena, Part II, Wear 6, pp. 169-90.
4. Bourgoyne, A.T. 1989, " Experimental Study of Erosion in Diverter Systems Due to Sand Production," SPE/IADC 18716 Drilling Conference, New Orleans, Louisiana, pp. 807-816.
5. Bourgoyne, A.T. , Casariego, V., and Kelly, O.A. 1993, "Analysis of Injecting Water and/or a Friction Reducing Agent as a Means of Reducing Diverter Erosion during Diverter Operations,"1993 OCS Study MMS.

6. Finnie, I. **1960**, "Erosion of Surfaces by Solid Particles," Wear 3, pp. 87-103.
7. Goodwin, J.E., Sage, W., and Tilly, G.P. **1969** " Proceedings of Institute of Mechanical Engineers " , Volume 184, pp. 279-292.
8. Ives, L.K., and Ruff, A.W. **1978**, Wear 46, pp. 149-162.
9. Johnson, P.W. **1987**, "Experimental Study of Erosion in a Model Diverter System," A Thesis, Louisiana State University.
10. Rohleder, Stephen A. **1985**, "Erosional Aspects of Diverter Designs," A Thesis, Louisiana State University.

APPENDIX

Table A1 : Effect of Angle of Impact on Specific Erosion Factor

Material : Steel Flat Plate ASTM-A36 Specification

Sand Grain Size # 16-40 mesh

Air Pressure Upstream of Critical Prover : 90 psig

Angle of Impact	Sand Flow Rate (m ³ /sec)	Air Flow Rate (m ³ /sec)	F _d	Specific Erosion Factor (gm/kg)	Observed Erosion Rate (in/min)	Apparent Specific Erosion Factor (gm/kg)
90	9.927 E-06	0.01896	0.9994767	0.25213	0.0234	0.0629
80	1.038 E-05	0.01920	0.9994595	0.24468	0.0240	0.0640
70	1.009 E-05	0.01954	0.9994835	0.26032	0.0322	0.0661
60	1.038 E-05	0.01930	0.9994624	0.28224	0.0388	0.0737
50	1.027 E-05	0.01937	0.9994701	0.33681	0.0394	0.0870
45	1.067 E-05	0.01947	0.9994525	0.34071	0.0410	0.0914
40	1.009 E-05	0.01947	0.9994817	0.37615	0.0410	0.0955
35	1.061 E-05	0.01933	0.9994515	0.40062	0.0432	0.1069
32	1.049 E-05	0.01872	0.9994396	0.41336	0.0447	0.1092
30	1.027 E-05	0.01933	0.9994691	0.43602	0.0470	0.1126
28	9.870 E-06	0.01906	0.9994825	0.44729	0.0370	0.1111
25	1.044 E-05	0.01886	0.9994467	0.42164	0.0328	0.1107
20	1.038 E-05	0.01954	0.9994690	0.40821	0.0260	0.1066

Table A2 : Effect of Sand Flow Rate on Specific Erosion Factor

Material : Steel Flat Plate ASTM-A36 Specification

Sand Grain Size # 16-40 mesh

Air Pressure Upstream of Critical Prover : 90 psig

Angle of Impact	Sand Flow Rate (m ³ /sec)	Air Flow Rate (m ³ /sec)	F _d	Specific Erosion Factor (gm/kg)	Observed Erosion Rate (in/min)	Apparent Specific Erosion Factor (gm/kg)
30	5.434 E-05	0.01377	0.9960704	0.13007	0.0524	0.03832
30	2.687 E-05	0.01745	0.9984625	0.24901	0.0520	0.07692
30	2.139 E-05	0.01809	0.9988187	0.26219	0.0476	0.08843
30	2.065 E-05	0.01702	0.9987880	0.26978	0.0476	0.09161
30	1.820 E-05	0.01782	0.9989801	0.29025	0.0460	0.10046
30	1.192 E-05	0.01831	0.9993493	0.40610	0.0412	0.13734

Table A3 : Effect of Sand Grain Size on Specific Erosion Factor

Material : Steel Flat Plate ASTM-A36 Specification
 Angle of Impact : 30 Degrees
 Air Pressure at Upstream of Critical Prover : 90 psig

Sand Grain Size	Sand Flow Rate	Air Flow Rate	F_d	Specific Erosion Factor	Observed Erosion Rate	Apparent Specific Erosion Factor
(Mesh #)	(m ³ /sec)	(m ³ /sec)		(gm/kg)	(in/min)	(gm/kg)
16-40	2.065 E-05	0.01702	0.998788	0.26978	0.0476	0.09161
35-80	2.008 E-05	0.01845	0.998913	0.28559	0.0496	0.09929
80-120	2.002 E-05	0.01773	0.998872	0.18591	0.0392	0.07900
200	2.225 E-05	0.01805	0.998769	0.20350	0.0450	0.08193

Table A4 : Effect of Varying Distance Between Nozzle and Target on Specific Erosion Factor

Material : Steel Flat Plate ASTM-A36 Specification
 Angle of Impact : 30 Degrees
 Air Pressure at Upstream of Critical Prover : 90 psig
 Sand Grain Size # 16-40 mesh

Distance of Nozzle from Target	Sand Flow Rate	Air Flow Rate	F_d	Specific Erosion Factor	Observed Erosion Rate	Apparent Specific Erosion Factor
(inches)	(m ³ /sec)	(m ³ /sec)		(gm/kg)	(in/min)	(gm/kg)
0	1.169 E-05	0.019407	0.9993976	0.46242	0.0420	0.14274
0.433	1.152 E-05	0.019202	0.9994001	0.52386	0.0450	0.15521
1.432	1.198 E-05	0.019474	0.9993851	0.51650	0.0472	0.15659
2.057	1.181 E-05	0.019133	0.9993831	0.51014	0.0366	0.12318
2.432	1.169 E-05	0.019474	0.9993998	0.49898	0.0318	0.10807
2.932	1.169 E-05	0.018989	0.9993844	0.43446	0.0272	0.09244

Table A5 : Comparison of Specific Erosion Factors of Erosion Resistant Materials at Thirty Degree Angle of Impact

Material : Erosion Resistant Coupons
Sand Grain Size # 16-40 mesh

Coupon	Sand Flow Rate (m ³ /sec)	Air Flow Rate (m ³ /sec)	F _q	Specific Erosion Factor (gm/kg)	Observed Erosion Rate (in/min)	Apparent Specific Erosion Factor (gm/kg)
LC36	2.065 E-05	0.01702	0.998788	0.26978	0.0476	0.09161
SArNi	2.487 E-05	0.01961	0.9987335	0.29327	0.0410	0.06551
GMNi	2.487 E-05	0.01982	0.9987465	0.27557	0.0436	0.06967
LCSS	2.493 E-05	0.01858	0.9986603	0.26233	0.0378	0.06026
ST21K	2.350 E-05	0.01879	0.9987506	0.27771	0.0352	0.05952
ST6K	2.407 E-05	0.01880	0.9987245	0.23717	0.0308	0.05085

Material : Erosion Resistant Coupons
Sand Grain Size # 35-80 mesh

Coupon	Sand Flow Rate (m ³ /sec)	Air Flow Rate (m ³ /sec)	F _q	Specific Erosion Factor (gm/kg)	Observed Erosion Rate (in/min)	Apparent Specific Erosion Factor (gm/kg)
LC36	2.008 E-05	0.01845	0.9989130	0.28559	0.0476	0.09929
SArNi	1.957 E-05	0.01926	0.9989853	0.40042	0.0512	0.10400
GMNi	1.934 E-05	0.01906	0.9989865	0.38043	0.0452	0.09289
LCSS	1.939 E-05	0.01996	0.9990294	0.33457	0.0644	0.13196
ST21K	1.917 E-05	0.01989	0.9990374	0.32871	0.0250	0.05183
ST6K	1.751 E-05	0.01989	0.9991202	0.34971	0.0304	0.06899

Material : Erosion Resistant Coupons
Sand Grain Size # 80-120 mesh

Coupon	Sand Flow Rate (m ³ /sec)	Air Flow Rate (m ³ /sec)	F _q	Specific Erosion Factor (gm/kg)	Observed Erosion Rate (in/min)	Apparent Specific Erosion Factor (gm/kg)
LCS36	2.002 E-05	0.01773	0.998872	0.18591	0.0392	0.07900
SArNi	2.088 E-05	0.01870	0.9988846	0.20841	0.0300	0.05798
GMNi	2.071 E-05	0.01820	0.9988634	0.20102	0.0270	0.05261
LCSS	2.031 E-05	0.01815	0.9988824	0.17339	0.0244	0.04848
ST21K	2.099 E-05	0.01818	0.9988499	0.19282	0.0220	0.04240
ST6K	2.100 E-05	0.01818	0.9988468	0.17253	0.0196	0.03767

Table A6 : Comparison of Specific Erosion Factors of Erosion Resistant Materials at Ninety Degrees of Impact Angle

Material : Erosion Resistant Coupons
Sand Grain Size # 16-40 mesh

Coupon	Sand Flow Rate (m ³ /sec)	Air Flow Rate (m ³ /sec)	F _d	Specific Erosion Factor (gm/kg)	Observed Erosion Rate (in/min)	Apparent Specific Erosion Factor (gm/kg)
LC36	9.927 E-05	0.01896	0.9994767	0.25213	0.0330	0.0629
SArNi	2.447 E-05	0.01899	0.9987132	0.14645	0.0240	0.03397
LCSS	2.396 E-05	0.01926	0.9987578	0.20156	0.0330	0.05474
ST6K	2.419 E-05	0.01926	0.9987460	0.15390	0.0148	0.02431
ST21K	2.476 E-05	0.01906	0.9987029	0.16407	0.0222	0.03563
GMNi	2.265 E-05	0.01913	0.9988176	0.22212	0.0256	0.04429

Material : Erosion Resistant Coupons
Sand Grain Size # 35-80 mesh

Coupon	Sand Flow Rate (m ³ /sec)	Air Flow Rate (m ³ /sec)	F _d	Specific Erosion Factor (gm/kg)	Observed Erosion Rate (in/min)	Apparent Specific Erosion Factor (gm/kg)
SArNi	1.934 E-05	0.01954	0.9990113	0.14307	0.0180	0.03699
LCSS	1.900 E-05	0.03816	0.9995025	0.24561	0.0292	0.06109
ST6K	1.774 E-05	0.01920	0.9990768	0.19706	0.0170	0.03808
ST21K	1.785 E-05	0.01947	0.9990839	0.21904	0.0220	0.04897
GMNi	1.911 E-05	0.01947	0.9990195	0.19413	0.0176	0.03666

Material : Erosion Resistant Coupons
Sand Grain Size # 80-120 mesh

Coupon	Sand Flow Rate (m ³ /sec)	Air Flow Rate (m ³ /sec)	F _d	Specific Erosion Factor (gm/kg)	Observed Erosion Rate (in/min)	Apparent Specific Erosion Factor (gm/kg)
SArNi	1.957 E-05	0.01771	0.9988964	0.06813	0.0100	0.02062
LCSS	2.082 E-05	0.01852	0.9988768	0.09241	0.0102	0.01976
ST6K	2.065 E-05	0.01821	0.9988675	0.07186	0.0064	0.01250
ST21K	2.099 E-05	0.01852	0.9988676	0.07787	0.0060	0.01153
GMNi	1.997 E-05	0.01870	0.9989333	0.07999	0.0050	0.01010